

U.C. Marx  
J. Klodt  
M. Meyer  
H. Gerlach  
P. Rösch  
W.-G. Forssmann  
K. Adermann

# One peptide, two topologies: structure and interconversion dynamics of human uroguanylin isomers

## Authors' affiliations:

U.C. Marx, Niedersächsisches Institut für Peptid-Forschung (IPF), Hannover, Germany, and Lehrstuhl für Struktur und Chemie der Biopolymere, Universität Bayreuth, Bayreuth, Germany.

J. Klodt, M. Meyer, W.-G. Forssmann, and K. Adermann, Niedersächsisches Institut für Peptid-Forschung (IPF), Hannover, Germany.

H. Gerlach, Lehrstuhl für Organische Chemie II, Universität Bayreuth, Bayreuth, Germany.

P. Rösch, Lehrstuhl für Struktur und Chemie der Biopolymere, Universität Bayreuth, Bayreuth, Germany.

## Correspondence to:

Dr. Knut Adermann  
Niedersächsisches Institut für Peptid-Forschung (IPF)  
Feodor-Lynen-Strasse 31  
D-30625 Hannover, Germany  
Phone: int +49-511-5466262  
Fax: int +49-511-5466102  
E-mail: knutadermann@compuserve.com

## Dates:

Received 23 January 1998  
Revised 2 March 1998  
Accepted 21 March 1998

## To cite this article:

Marx, U.C., Klodt, J., Meyer, M., Gerlach, H., Rösch, P., Forssmann, W.-G., Adermann, K. (1998) One peptide, two topologies: structure and interconversion dynamics of human uroguanylin isomers. *J. Peptide Res.* 52, 229–240.

Copyright © Munksgaard 1998

ISSN 1397-002X

**Key words:** guanylin; heat-stable enterotoxin; isomerization; solution structure; topological stereoisomer; uroguanylin

**Abstract:** The peptide hormone uroguanylin stimulates chloride secretion via activation of intestinal guanylyl cyclase C (GC-C). It is characterized by two disulfide bonds in a 1–3/2–4 pattern that causes the existence of two topological stereoisomers of which only one induces intracellular cGMP elevation. To obtain an unambiguous structure-function relationship of the isomers, we determined the solution structure of the separated uroguanylin isoforms using NMR spectroscopy. Both isomers adopt well-defined structures that correspond to those of the isomers of the related peptide guanylin. Furthermore, the structure of the GC-C-activating uroguanylin isomer A closely resembles the structure of the agonistic *Escherichia coli* heat-stable enterotoxin. Compared with guanylin isomers, the conformational interconversion of uroguanylin isomers is retarded significantly. As judged from chromatography and NMR spectroscopy, both uroguanylin isoforms are stable at low temperatures, but are subject to a slow pH-dependent mutual isomerization at 37°C with an equilibrium isomer ratio of approximately 1:1. The conformational exchange is most likely under the sterical control of the carboxy-terminal leucine. These results imply that GC-C is activated by ligands exhibiting the molecular framework corresponding to the structure of uroguanylin isomer A.

**Abbreviations:** cGMP, cyclic 3',5'-guanosine monophosphate; Clean-TOCSY, TOCSY with suppression of NOESY-type cross peaks; DG, distance geometry; DQF-COSY, double-quantum filtered COSY; DSS, 2,2-dimethyl-silapentane-5-sulfonic acid; GC-C, guanylyl cyclase C; JR-NOESY, 2D NOESY spectrum acquired with a jump-return observe pulse; MD, molecular dynamics; NMR, nuclear magnetic resonance; NOE, nuclear Overhauser effect, also used for NOESY cross peak; NOESY, NOE spectroscopy; RMSD, root-mean-

square deviation; SA, simulated annealing; ST, *Escherichia coli* heat-stable enterotoxin; STaR, *E. coli* heat-stable enterotoxin receptor; TOCSY, total correlation spectroscopy; TPPI, time-proportional phase incrementation.

Uroguanylin is a small mammalian peptide hormone that is known to be involved in the regulation of epithelial water and electrolyte transport. It is related structurally and functionally to the agonistic peptide guanylin (1–3). A target protein for uroguanylin is guanylyl cyclase C (GC C), also known as an *Escherichia coli* heat-stable enterotoxin (ST) receptor (STaR) (4, 5). Activation of GC-C increases intracellular production of cyclic guanosine monophosphate (cGMP) (3, 6), thereby stimulating cGMP dependent protein kinase type II (cGKII) (7, 8). cGKII in turn is responsible for chloride secretion by the activation of cystic fibrosis transmembrane conductance regulator (CFTR), resulting in intestinal fluid and chloride accumulation (9).

Uroguanylin of which different molecular forms were identified in urine (3, 6), blood (10, 11), and the intestine (12, 13) is related closely to guanylin on the level of primary structures (Fig. 1). Both peptides are characterized by two disulfide bonds in relative positions 1–3 and 2–4, which are crucial for biological activity (2, 14, 15). The disulfides are located within a short sequence of 12 amino acid residues. This structural element leads to the existence of two distinct topological isoforms of each peptide (15, 16). The enterotoxin ST exhibits an equivalent pattern of disulfides, but has an additional disulfide loop which may enhance its conformational rigidity (17–19). In binding assays, both peptides compete with ST for their common receptor GC C. However, the endogenous peptides are less potent activators of GC-C than ST is (10, 20, 21).

The topological stereoisomers of guanylin and uroguanylin exhibit the same cysteine connectivity, but are conformationally distinct molecules. A synthetic derivative of 13

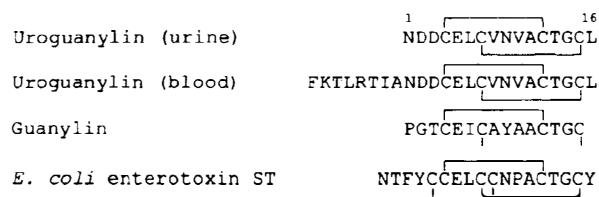


**Figure 1.** Amino acid sequences and disulfide pattern of GC-C activating peptides. The primary structures of human uroguanylin and guanylin are shown. ST is from a human strain of *E. coli* (41) with the GC C binding and toxic domain located between the outer cysteine residues.

amino acids of guanylin and a 22-residue guanylin fragment produced by tryptic digestion of the recombinant pro-hormone consist of two species each (molar ratio, 1:1) which can not be separated (16). One of those isoforms (A) adopts a well-defined structure with a right handed spiral conformation similar to that of ST obtained from X-ray crystallography (22). The second isoform (B) adopts a less well-defined left-handed spiral conformation, and therefore, is suggested to have a lower affinity to the receptor GC C (16). This isomerism was confirmed by NMR spectroscopy for guanylin containing 17 amino acids (23). Two components were observed clearly during high-performance liquid chromatography (HPLC) analysis for this peptide only and the smaller guanylin of 15 residues. Rapid interconversion between the two compounds, however, prevented the characterization of the isolated molecular species (15, 23). Recently, the synthesis of two different topological isoforms of human uroguanylin was reported (24). Polyclonal antisera against these isoforms were used to detect uroguanylin and its corresponding 10-kDa prohormone in urine and plasma (11). Although not shown on the structural level of the peptides, this finding suggests that both stereoisomers of uroguanylin are present in the body. In addition to the possible existence of other specific receptors for the GC-C-active isomer of uroguanylin, nothing is known about the structure and function of the peptide's B form that does not cause an increase of intracellular cGMP.

The purpose of this study was to establish an unambiguous structure-activity relationship of uroguanylin stereoisomers by combining the NMR-spectroscopical structure determination with the GC-C-activating potential and the dynamical characteristics of uroguanylin isomers. The results obtained are a prerequisite to model the interaction of ligands with the target protein GC-C with respect to the inhibition of GC-C activity and enterotoxic infections.

## Experimental Procedures

### Peptide synthesis, analytical chromatography and polarimetry

Uroguanylin-16 and uroguanylin-24 were synthesized on a preloaded Tentagel-S-PHB-LeuFmoc resin (Rapp Polymere). Disulfides of uroguanylin-16 were introduced selectively by air oxidation of Cys4 and Cys12 followed by iodine treatment of acetamidomethyl-protected cysteine residues 7 and 15. After formation of the second disulfide, two stereoisomers were obtained and separated by reversed-phase HPLC at a temperature of 15°C. Uroguanylin-24 was prepared cor

respondingly. A detailed synthetic procedure was reported recently by Klodt *et al.* (15). The identity of synthetic peptides was confirmed by electrospray mass spectrometry and sequence analysis by Edman degradation. For the cGMP T84 cell assay, synthetic peptides were used according to the net peptide content as determined by amino acid analysis. The HPLC study of the mutual conversion of purified uroguanylin isoforms was carried out using a C18 column (Nucleosil C18 PPN, Macherey & Nagel, 2 × 250 mm, 5 μm, 100 Å, buffer A: 0.06% trifluoroacetic acid; buffer B: 0.06% trifluoroacetic acid in 80% acetonitrile; flow rate, 0.2 mL/min; UV detection at 215 nm; peptide concentration, 1 μg/10 μL). Polarimetry was carried out on a Perkin-Elmer 241 polarimeter. Sample concentration was 1 mg/mL (0.60 mM) using 10-cm cells. The optical rotation at 18°C was detected at 589 nm (Na), 578 nm (Hg), 546 nm (Hg), 436 nm (Hg) and 365 nm (Hg). Starting from pure isoforms the changes of the optical rotation were examined for 120 h. For the first 24 h, the samples were stored at room temperature; from 24 to 120 h, the samples were incubated at 37°C between the measurements.

### NMR spectroscopy

Two-dimensional NMR spectra were obtained on commercial Bruker AMX600 and AMX400 spectrometers at 11°C by standard methods (25, 26). Peptide concentrations were: 1.5 mM, pH 3.9 (uroguanylin-24); 4.9 mM, pH 3.3 (uroguanylin-16, isomer A); and 4.1 mM, pH 3.3 (uroguanylin-16, isomer B), in H<sub>2</sub>O/D<sub>2</sub>O (9:1, v/v, 500 μL). The H<sub>2</sub>O resonance was presaturated by continuous coherent irradiation at the H<sub>2</sub>O resonance frequency before the reading pulse, except the JR-NOESY. The sweep widths in  $\omega_1$  and  $\omega_2$  were 9 ppm (5434.8 Hz on AMX600 and 3623.2 Hz on AMX400 spectrometer). Quadrature detection was used in both dimensions with the time proportional phase incrementation (TPPI) technique in  $\omega_1$ . In  $\omega_2$  4000 data points were collected, and 512 data points in  $\omega_1$ . Zero filling to 1000 data points was used in  $\omega_1$ . Spectra were multiplied with a squared sinebell function phase shifted by  $\pi/4$ ,  $\pi/3$ , and  $\pi/2$  for the NOESY spectra, by  $\pi/4$  for the Clean-TOCSY and the DQF-COSY spectra. Baseline and phase correction of the sixth order was used. Data were evaluated on X-Window workstations with the NDee program package (Software Symbiose, Bayreuth). For the sequence-specific assignment of spin systems and the evaluation of the NOESY distance constraints for the peptides, data from the following 600 MHz spectra were used: DQF-COSY, Clean-TOCSY with a mixing time of 80 msec, NOESY with a mixing time of 200 msec and JR-NOESY with

a mixing time of 200 msec. For estimation of the coupling constants, DQF-COSY spectra were recorded with 8000 data points in  $\omega_2$  and 512 data points in  $\omega_1$  and were processed without window function. Coupling constants were measured between the antiphase peaks of the resonances using a Lorentzian function for peak fitting. The time dependent 1D NMR spectra were obtained from the AMX400 spectrometer (400 MHz) at 25°C. For the first 24 h, samples were stored at room temperature between the measurements; from 24 to 92 h, samples were stored at 37°C.

### Structure calculations and analysis

The total number of nontrivial unambiguous NOESY cross peaks used for structure calculation was 84 for the A form of uroguanylin-16 and 69 for the B form (Table 1). These cross peaks were divided into three groups according to their relative intensities: strong, 0.2 to 0.3 nm; medium, 0.2 to 0.4 nm; weak, 0.2 to 0.5 nm. In a pseudoatom approach, 0.05 nm was added to the upper distance limit for distances involving unresolved methyl or methylene proton resonances. Also included by an iterative strategy were 5  $\phi$  and 3  $\chi^1$  dihedral angle restraints for isomer A and 4  $\phi$  and 2  $\chi^1$  dihedral angle restraints for the B form. Deviations of 30° from the calculated angles were allowed in the cal-

Table 1. Energy contributions, deviations from standard geometry, and NCE and X-PLCE statistics of uroguanylin-16

	Isomer A	Isomer B
<sup>15</sup> N- <sup>1</sup> H distance restraints		
Total NCE number	84	69
$\langle r^{-1} \rangle = 0$	8	4
$\langle r^{-1} \rangle = 1$	80	55
$\langle r^{-1} \rangle = 2$	8	5
$\langle r^{-1} \rangle = 3$	1	1
$\langle r^{-1} \rangle = 4$	0	1
$\langle r^{-1} \rangle = 5$	7	3
Dihedral angle restraints		
$\phi$	5	4
$\chi^1$	3	2
Average energies <sup>a</sup> (kJ/mol)		
$E_{\text{total}}$	72.37	82.83
$E_{\text{bond}}$	1.46	2.54
$E_{\text{angle}}$	54.11	55.92
$E_{\text{torse}}$	7.00	2.53
$E_{\text{vdw}}$	4.64	2.72
$E_{\text{elec}}$	5.85	13.38
$E_{\text{hydro}}$	12.884	0.219
Deviations from standard geometry		
Bonds	$1.25 \times 10^{-3}$ nm	$1.87 \times 10^{-3}$ nm
Angles	0.470°	0.478°
NCEs	$1.68 \times 10^{-3}$ nm	$2.87 \times 10^{-3}$ nm
Dihedral	0.014°	0.078°
RMSD among backbone structures (nm)		
Whole peptide	0.129	0.115
Cys4-Cys15	0.075	0.083

a.  $E_{\text{total}}$ : total energy;  $E_{\text{bond}}$ : covalent bond energy term;  $E_{\text{angle}}$ : bond angle energy term;  $E_{\text{torse}}$ : improper angle energy term;  $E_{\text{vdw}}$ : van der Waals energy;  $E_{\text{elec}}$ : effective NCE energy term resulting from a square-well potential function;  $E_{\text{hydro}}$ : dihedral angle energy term. All calculations were carried out using the standard X-PLCE force field and energy terms. The values are the mean of 10 defined structures of each peptide.

ulation without penalty. Structure calculations were performed using a modified *ab initio* SA protocol with an extended version of X-PLOR 3.1 program package (27). The structure calculation included floating assignments of prochiral groups (28) and a reduced presentation for nonbonded interactions for part of the calculation (29) to increase efficiency. The calculation strategy is similar to those described previously (30, 31). Structure parameters were extracted from the standard files *parallhdg.pro* and *topallhdg.pro* of X-PLOR V3.840 (27). The disulfide bonds were included explicitly. For each fragment, 30 structures were calculated and 10 structures for each isoform were selected with the criterion of the lowest overall energy for further characterization. SYBYL 6.0 (TRIPOS), RASMOL V. 2.6 (32) and MOLSCRIPT (33) were used for visualization of the structure data. To elucidate the stability of the structures, we calculated local RMSD using SYBYL 6.0 as well as XPLOR 3.1. The geometry of the structures was analyzed using PROCHECK (34), PROMOTIF (35) and XPLOR 3.1.

#### cGMP T84 cell assay

Synthetic peptides were tested to assess the specific GC-C-stimulating potency as described previously (e.g. 10, 21). T84 cells were preincubated with 1 mM isobutylmethylxanthine for 5 min. Then, peptides were added to the medium in a concentration range of  $10^{-9}$  to  $10^{-6}$  M and cells were incubated for 60 min. Incubation was stopped by removal of medium and addition of ice cold ethanol. The amount of intracellular cGMP induced by the peptides was determined using a specific radioimmunoassay (36).

## Results and Discussion

The isomers of uroguanylin-16 and the amino-terminally extended uroguanylin-24 were synthesized and separated using standard chromatography techniques as described under "Experimental Procedures". The GC-C-activating and earlier eluting compound during HPLC is referred to as isomer A.

#### Chemical shift analysis

With very little resonance overlap in the 2D NMR spectra of the separated isoforms of uroguanylin-16 (Fig. 2), the sequence-specific assignment of each species could be performed by standard methods (26, Table 2). The amide proton chemical shifts of Cys7, Val8, Cys12 and Thr13 dif-

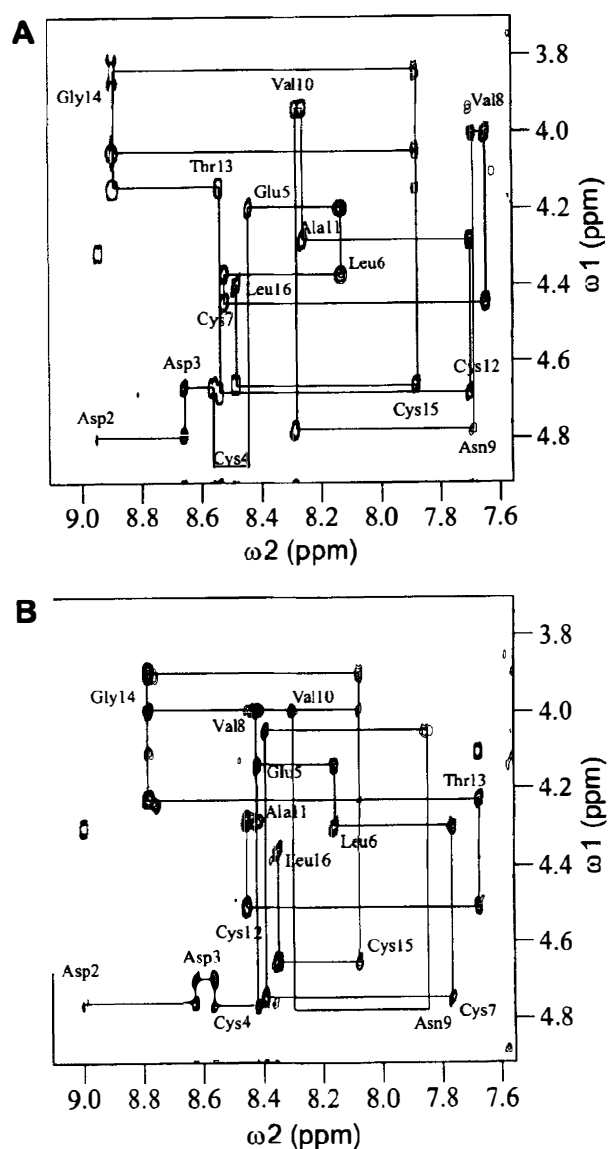


Figure 2. NOESY spectra (200 msec) of uroguanylin 16 isomers. Fingerprint region of (A) isomer A and (B) of isomer B. The intraresidual cross peaks between the amide and  $\alpha$ -protons of each amino acid are labeled and the chain tracing along the sequence is indicated.

fer by up to 1 ppm between the two isoforms, indicating that the backbone folds in these regions are different (Fig. 3A). The differences in the chemical shifts of the  $\alpha$ -proton resonances with a maximum of 0.3 ppm are less significant, but obvious for the residues Cys7 and Cys12 (Fig. 3B). Amide proton chemical shifts of the first six and  $\alpha$ -proton chemical shifts of the first three residues are virtually identical for both isoforms, indicating that the backbone folds of the amino-terminus of both isoforms are similar. In the 2D NMR spectra of a 1:1 mixture of both isoforms of the  $\text{NH}_2$ -terminally extended uroguanylin-24 (data

Table 2.  $^1\text{H}$  chemical shifts and assignments for isomers A and B of uroguanylin-16<sup>a</sup>

Residue	Isomer A					Isomer B				
	NH	C $\alpha$ H	C $\beta$ H	C $\gamma$ H	Other	NH	C $\alpha$ H	C $\beta$ H	C $\gamma$ H	Other
Asp1		4.31	2.97		7.76, 7.05 (NH <sub>2</sub> )		4.31	3.61		7.76, 7.07 (NH <sub>2</sub> )
Asp2	8.94	4.73	2.93, 2.83			9.00	4.78	2.94, 2.87		
Asp3	8.66	4.67	2.93, 2.86			8.63	4.70	2.97, 2.85		
Cys4	8.58	4.88	3.38, 2.86			8.57	4.77	3.21, 3.13		
Gly5	8.44	4.20	2.99	2.48		8.42	4.14	2.07	2.48	
Ileu6	8.13	4.37	1.74, 1.62	1.56	0.90, 0.86 (C)	8.16	4.30	1.73, 1.65	1.56	0.93, 0.83 (C)
Cys7	8.52	4.45	3.32, 2.89			7.76	4.34	3.20		
Val8	7.65	4.00	2.12	0.92		8.39	4.05	2.18	0.95	
Arg9	7.69	4.78	3.04, 2.79		7.68, 6.95 (NH <sub>2</sub> )	7.85	4.78	2.92, 2.82		7.63, 7.03 (NH <sub>2</sub> )
Val10	8.28	3.94	2.22	0.98, 0.94		8.30	4.00	2.14	0.96	
Ala11	8.26	4.28	1.38			8.42	4.28	1.38		
Cys12	7.79	4.68	3.23			8.45	4.50	3.48, 3.17		
Thr13	8.54	4.15	4.15	1.23		7.67	4.23	4.11	1.17	
Gly14	8.90	4.05, 3.84				8.76	3.98, 3.90			
Cys15	7.88	4.66	3.08			8.07	4.65	3.45, 2.98		
Ileu16	8.48	4.40	1.67	1.65	0.91, 0.86 (C)	8.35	4.36	1.67	1.67	0.91, 0.86 (C)

<sup>a</sup> 11°C, pH 3.3, DSS as external standard, accuracy of  $\pm 0.01$  ppm.

not shown) only one set of spin systems was found for the residues Phe1 to Asp11, indicating that the 11 amino-terminal amino acids have the same conformation, most probably unstructured or extended, as judged from their C $\alpha$ -proton chemical shifts. For the 13 carboxy terminal amino acids, an unambiguous and independent assignment of resonances of the A and B forms was possible because of clear differences in the chemical shifts of both isoforms. The backbone chemical shift values of the last 13 amino acids comprising the Cys-rich region of uroguanylin-16 and -24 differ by less than 0.08 ppm for the corresponding isoforms with one exception, indicating that the isoforms of uroguanylin 24 most probably have a tertiary fold which closely resembles the corresponding isoforms of uroguanylin-16. Thus, the additional 8 amino acids at the amino terminus of uroguanylin-24 apparently do not influence the global fold of the backbones of the two isoforms.

#### Structure calculation and analysis of uroguanylin-16 isoforms

Eighty-four and sixty-nine distance restraints from the 200 msec-NOESY spectra at 11°C were collected for uroguanylin-16 isoforms A and B and were used together with 8 and 6 dihedral restraints, respectively, in restrained MD calculations (Table 1). For structure calculations of both isoforms, a modified *ab initio* simulated annealing (SA) pro-

cedure (27) was used with explicit inclusion of disulfide bonds. None of the ten selected structures shows NOE violations more than 0.03 nm, and no structure has angle violations more than 5°. Although only a few nonsequential NOEs were assigned, and no typical NOEs and no consecutive  $^3J_{\text{NH}\alpha\text{H}}$  coupling constants for any regular secondary structure element were found, the NMR data were sufficient to define well structured global folds for both isoforms. The well-defined global fold of the region from Cys4 to Cys15 is reflected by the low backbone root-mean square deviation (RMSD) of 0.075 nm for the A form and 0.063 nm for the B form (Fig. 4A). The structures of the isoforms A and B of uroguanylin are rather different: the backbone RMSD between the average structures of the A and B forms from residue Cys4 to Cys15 is 0.46 nm. For each fragment, the ten final structures have been deposited in the Brookhaven Protein Databank (accession numbers 1UYA and 1UYB).

The structure of the A form of uroguanylin-16 contains three loops, Cys4 to Cys7, Cys7 to Cys12 and Cys12 to Cys15. These loops are arranged in a right-handed spiral which is stabilized by disulfide bonds Cys4-Cys12 and Cys7-Cys15 (Fig. 4B, C). A view along the spiral axis shows that the connected cysteines are in line after one complete spiral turn. The three amino-terminal amino acids are unstructured. No elements of regular secondary structure were

# Explore Litigation Insights

Docket Alarm provides insights to develop a more informed litigation strategy and the peace of mind of knowing you're on top of things.

## Real-Time Litigation Alerts



Keep your litigation team up-to-date with **real-time alerts** and advanced team management tools built for the enterprise, all while greatly reducing PACER spend.

Our comprehensive service means we can handle Federal, State, and Administrative courts across the country.

## Advanced Docket Research



With over 230 million records, Docket Alarm's cloud-native docket research platform finds what other services can't. Coverage includes Federal, State, plus PTAB, TTAB, ITC and NLRB decisions, all in one place.

Identify arguments that have been successful in the past with full text, pinpoint searching. Link to case law cited within any court document via Fastcase.

## Analytics At Your Fingertips



Learn what happened the last time a particular judge, opposing counsel or company faced cases similar to yours.

Advanced out-of-the-box PTAB and TTAB analytics are always at your fingertips.

## API

Docket Alarm offers a powerful API (application programming interface) to developers that want to integrate case filings into their apps.

## LAW FIRMS

Build custom dashboards for your attorneys and clients with live data direct from the court.

Automate many repetitive legal tasks like conflict checks, document management, and marketing.

## FINANCIAL INSTITUTIONS

Litigation and bankruptcy checks for companies and debtors.

## E-DISCOVERY AND LEGAL VENDORS

Sync your system to PACER to automate legal marketing.